Korean J. Chem. Eng., 32(4), 609-616 (2015)
DOI: 10.1007/s11814-014-0244-7

pISSN: 0256-1115
eISSN: 1975-7220

Pressure drop and thermal performance of CuO/ethylene glycol (60%)-water (40%) nanofluid in car radiator

Pourfarhang Samira, Zeinali Heris Saeed†, Shokrgozar Motahare, and Kahani Mostafa

Chemical Engineering Department, Ferdowsi University of Mashhad, Mashhad, Iran
(*Received 26 May 2013 • accepted 24 August 2014*)

Abstract−We investigated the role of nanofluid in a special car radiator and the effect of its different volume concentrations on pressure drop and friction factor of fluid flow. A mixture of 60/40 ratio of ethylene glycol (EG) and distilled water was used as the host fluid and CuO nanoparticles were dispersed well to make stable nanofluids. The influence of nanofluid concentrations on pressure drop was evaluated in the radiator at three different inlet fluid temperatures (35, 44, 54 °C). The results demonstrated that the presence of nanoparticles caused an increase in nanofluid pressure drop, which was intensified by increasing nanoparticle concentration as well as decreasing temperature of inlet fluid. A new empirical equation for prediction of nanofluid pressure drop through the radiator was developed as well. Also, with increasing the flow rate, the performance index increased and indicated that application of nanofluid in higher flow rate was affordable.

Keywords: Radiator Coolant, Nanofluid, Pressure Drop, Friction Factor, Performance Index

INTRODUCTION

Nanofluids contain particles with nanometer dimensions suspended in liquids (mainly, conventional heat transfer fluids) that considerably enhance heat transfer performance of fluids [1]. Using a nanofluid as the heat transfer working fluid has gained much attention in recent years [2-11]. In addition, with the development of nanotechnology, the design of automobiles that have high energy efficiency and low depreciation has been highly considered in recent years. Considering the urgent need to reduce the dimensions and weight of heat transfer systems in various industries such as the transportation industry, many researchers have recently worked to develop ways of enhancing heat transfer rate. One of these ways is to replace the conventional heat transfer fluid systems with nanofluids [12,13]. The result of a literature review about using nanofluid as a motor coolant indicates heat transfer improvement in heat exchangers such as car radiators by nanofluids, but the presence of nanoparticles, because of increasing fluid viscosity, intensifies the pressure drop and pumping power in the heat transfer system. Many researchers believe that the overall system performance would be reduced if the undesired effects of pressure drop increment were higher than the desired effect of heat transfer enhancement [7].

The existence of solid particles in traditional heat transfer fluids may be affected by a variety of agents, including type and size of particles, which increase viscosity and thus increase pressure drop [14-17]. Rea et al. [18] investigated heat transfer and pressure drop of Al_2O_3/water and zirconium/water nanofluids in laminar flow inside a horizontal tube. They highlighted that the heat transfer coefficient increased with increasing concentration of nanoparticles. Also, they reported about 7.2-times increase in nanofluid pressure drop for a given flow velocity and channel geometry compared to pure water. Kumar et al. [19] measured the heat transfer and friction factor of a shell and helically coiled tube heat exchanger using Al_2O_3/water nanofluid at 0.1-0.8% particle volume concentration. They reported that the addition of nanoparticles in base fluid leads to higher thermal conductivity and friction factor. Leong et al. [13] studied heat transfer features in a car radiator with Cu/EG nanofluids as a coolant and concluded that intensity of heat transfer increased with increasing volumetric concentration. In addition, 12.13% increment in pumping power was observed for 2% addition of copper nanofluids compared to base fluid.

The heat transfer and pressure drop of TiO_2/water nanofluid at 0.2 vol% in a double-tube heat exchanger were studied by Duangthongsuk and Wongwises [20]. Their results presented about 6-11% increase in the convective heat transfer coefficient of nanofluid compared to pure water, considering the little penalty in pressure drop. Plus, Lee and Mudawar [21] discussed the effect of Al_2O_3 nanoparticles on pressure drop of nanofluid consisting of water as base fluid in micro-channel. The results showed that pressure drop of nanofluid was higher than that of pure fluid and increased with the increase of nanoparticle concentrations at the same Reynolds number. Also, experiments on the pressure drop of CuO/water nanofluid in a miniature plate heat exchanger with a modulated surface showed that the presence of nanoparticle caused a slight increase (less than 10%) in pressure drop [22]. An experimental study on convective boiling heat transfer and pressure drop of nanofluids and water flowing in a multichannel was done by Boudouh et al. [23].

Fotukian and Nasr Esfahany [24] investigated the convective heat transfer and pressure drop of dilute CuO/water nanofluids inside a circular tube under a turbulent flow condition. They em-

†To whom correspondence should be addressed.
E-mail: zeinali@ferdowsi.um.ac.ir

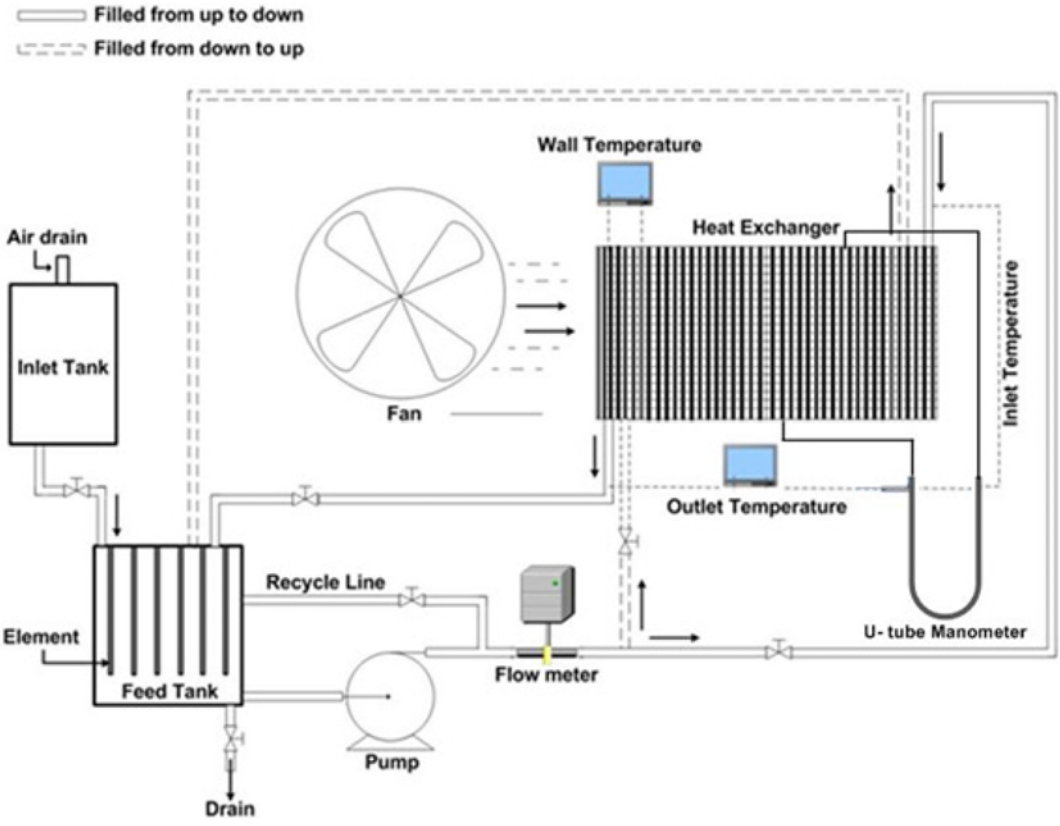

Fig. 1. Schematic of experimental setup.

phasized that addition of small amounts of nanoparticles to the base fluid can increase the heat transfer coefficient and pressure drop. The heat transfer performance and pressure drop of TiO_2-distilled water nanofluids flowing through a vertical pipe in an upward direction under a constant heat flux in both laminar and turbulent flow regimes was reported by He et al. [25]. Their results indicated that local heat transfer coefficient increased with increasing nanoparticle concentration in both laminar and turbulent flow regimes at a given Reynolds number and particle size. Moreover, pressure drop of the nanofluids was very close to that of the base fluid. Finally, to measure the pressure drop and viscosity of nanofluid, Ko et al. [26] considered carbon nanotubes in distilled water through a horizontal tube. Their results clearly indicated that the nanofluids prepared by acid treatment (TCNT) had much smaller viscosity than the ones made by surfactant (PCNT). Besides, under laminar flow conditions, friction factor of the PCNT nanofluids was much higher than that of the TCNT nanofluids. Moreover, both nanofluids showed larger friction factors than the base fluid. In contrast, under turbulent flow conditions, the friction factor of both nanofluids became similar to that of the base fluids as the flow rate increased.

In the present study, pressure drop and friction factor of EG (60%)-water (40%)/CuO nanofluid in the radiator of PRIDE (PRIDE is a brand of car commonly usedd in Iran) were investigated. The CuO nanoparticles (60 nm) were added to base fluid to study the effects of important parameters on pressure drop and thermal performance index of nanofluid flow in the PRIDE radiator.

EXPERIMENTAL SYSTEM AND PROCEDURE

The experimental setup for measuring pressure drop in the PRIDE radiator is shown schematically in Fig. 1. The experimental system consisted of a closed path of nanofluid. The working fluid, after being warmed in a feed reservoir, was pumped into the radiator using 2.0 cm inner diameter three-layer tubes and was cooled while passing through the radiator. After leaving the radiator, the working fluid was returned to the main tank. The size of feed reservoir was 22.5 liters and, in every feed, 25 liters nanofluid was nourished by a tank located on the top of the reservoir. To increase accuracy of the experiments, the radiator system should be completely closed, which was done using an air drain mounted on the top of the feeding repository. Moreover, to keep temperature of the working fluid between 30 and 60 °C, six electrical elements with the power of 18 kW and a controller were used. Three calibrated thermocouples (PT100-type) were inserted into the calming and mixing chamber of the flow at inlet and outlet of the radiator for measuring the bulk temperatures of working fluids, and also six K-type thermocouples were soldered at axial diameter on the outer surface of the radiator to measure wall temperatures. The accuracy of all thermocouples was ±0.1 °C of full scale. Due to very small thickness (2.0 mm) and very large thermal conductivity of the tubes, it was reasonable to equate inside temperature of the tube with the outside one.

The test section included a storage tank, a centrifugal pump, heating elements, flow meter, a forced draft fan, a cross flow heat ex-

changer and flow lines. The experimental setup was totally a closed system and worked under pressure (0.25 kPa) and the working fluid filled the whole storage tank in all the experiments. Additionally, the flow rate in the system was regulated by adjusting a globe valve on the recycle line. Three layer insulated tubes (Isopipe 0.75 in diameter) were applied as a connecting line. A flowmeter (Instrument Company LZT) was used to measure and manipulate the flow rate. When the flow rate was adjusted at beginning of experiments, it was monitored continually during the experiments. When it was fixed at our desired flow rate for at least 15 minute, the results were recorded. The accuracy of the flowmeter was around 2.0%.

The heat exchanger was a PRIDE radiator with 40 circular shaped cross section vertical tubes. All mechanical parts of the experimental setup were made of aluminum. For cooling the working fluid, a forced fan (Techno pars: 1,400 rpm) was installed behind the radiator. Air and fluid had indirect cross flow contact and heat exchanged between hot fluid flowing in the tube-side and air crossing the tube bundle. In addition, a U-tube manometer with carbon tetrachloride (CCl_4) as the manometer liquid was provided for determining pressure drop through the radiator. Constant velocity and temperature of the air through the experiments were considered in order to clearly investigate internal heat transfer. Also, the design of the system allowed filling the heat exchanger from up and down. In this study, all the experiments were run while the radiator was filled from up to down.

The experiments covered a range of flow rate from 4 to 8 liter/min (lpm) and the Reynolds number of 2000-8000. The required data for pressure drop and friction factor calculation were measured in a turbulent flow range and the nanofluid volume fraction of 0.05, 0.1, 0.3, 0.5 and 0.8 percent. Also, the effect of nanofluid concentrations on pressure drop was investigated under three different temperatures of input fluid for radiator.

PREPARING NANOFLUID AND EVOLUTION OF THERMOPHYSICAL PROPERTIES

We used CuO nanoparticles with average 60 nm diameters. Thermophysical properties of CuO nanoparticles are shown in Table 1. Fig. 2 shows the TEM (transmission electron microscopy) image of nanoparticles dispersed in the base fluid and reveals that the nanoparticles are spherical. To fill the experimental apparatus completely, a considerable amount of nanofluid was needed, so a three-step preparation method was used to prepare stable suspension of nanoparticles in the base fluid. At first, the required amount of nanoparticles was added to 10 liters of base fluid which was stirred for at least 14 hours by a high speed mechanical mixer (2,000 rpm); then, it was vibrated by an ultrasonic processor for 2 hours. During the experiments, the flow regime was considered turbulent and no settlement or deposition was observed. Also, the samples were kept in the stationary state for a month and were found quite stable without visually observable sedimentation. In addition, the density of prepared nanofluids was measured once nanofluid was prepared and also after 30 days. Reasonable agreement was achieved between the results which emphasizes the stable behavior of nanofluids without considerable sedimentation.

Table 1. Thermophysical properties of CuO nanoparticle

Grain size (nm)	60
Thermal conductivity (W $m^{-1}K^{-1}$)	69
Isobaric specific heat (J $kg^{-1}K^{-1}$)	535.6
Density (kgm^{-3})	6400

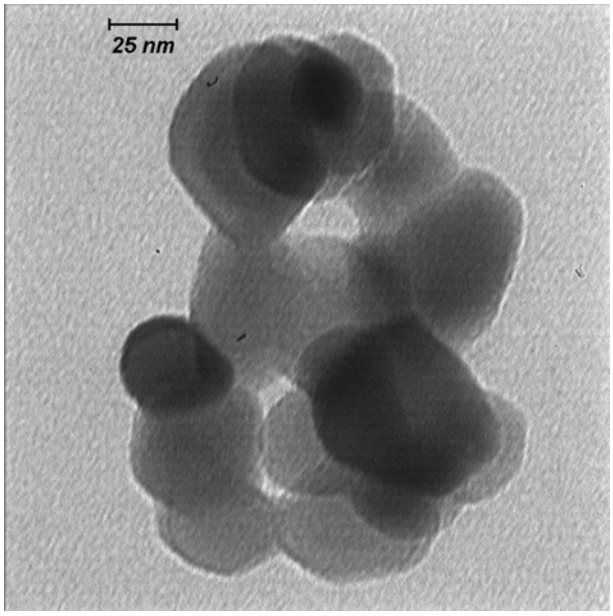

Fig. 2. TEM image of CuO nanoparticles.

In the present work, the base fluid was a blend of 60/40 EG and water. The values published by Sun and Teja [27] about thermophysical properties of various mixtures of water and EG were applied to calculate density and viscosity of fluid passing through the radiator. Table 2 shows some properties of pure EG and water and desired mixture at three tested temperatures. Thermophysical properties of nanofluid were calculated at the average bulk temperature. ρ_{nf} and μ_{nf} were calculated by the following equations [28,29]:

$$\rho_{nf}=\varphi\rho_p+(1-\varphi)\rho_{bf} \quad (1)$$

$$\mu_{nf}=\mu_{bf}(1+2.5\varphi) \quad (2)$$

Table 2. Density and viscosity of EG (60%) and water (40%) mixture at three different temperatures [27]

Thermophysical properties	Water (40 °C)	EG (40 °C)	The blend of 60/40 EG/water		
			T=35 °C	T=44 °C	T=54 °C
Density (kg/m^3)	992	1101	1093.6946	1088.04	1080.697
Viscosity (kg/m·s)	0.00065	0.0095	0.0007698	0.005707	0.004353

CALCULATING PRESSURE DROP AND FRICTION FACTOR

The pressure drop for nanofluid flow through the radiator at different volume concentrations of nanoparticles was calculated by the following relation:

$$\Delta P_{nf}(\exp)=\rho_{CCl_4} g \Delta h \quad (3)$$

in which is liquid (CCl_4) density inside the capillary tube, g is acceleration gravity (9.8 m/s^2) and is change in the liquid height inside the U-tube manometer. Note that nanofluids which were used in these experiments were dilute mixtures of solid-liquid and, since very small dimensions of nanoparticles were easily dispersed in that, it can be considered as a single fluid.

Theoretical relations for single phase fluid pressure drop and friction factor can be expressed as follows [13]:

$$\Delta P_{nf}(\text{th})=\frac{f_{nf}G^2 nL}{2\rho_{nf}D\beta} \quad (4)$$

$$f_{turb.}=0.0031\,Re_{nf}^{-0.26} \quad (5)$$

where f_{nf} is nanofluid friction factor under turbulent flow regime and G is mass velocity of fluid calculated using mass flow rate ($\dot{m}$) and cross section (A) as follows:

$$G=\frac{\dot{m}}{A} \quad (6)$$

The cross section area of working fluid flow can be calculated using the following equation:

$$A=A_{fr}\sigma \quad (7)$$

which A_{fr} is frontal area and σ is minimum free flow area/frontal area.

$$\varphi_t=\left(\frac{\mu}{\mu_w}\right)n \quad (8)$$

where μ_w is nanofluid viscosity in wall temperature. Nanofluid Reynolds number (Re_{nf}) were calculated as:

$$Re_{nf}=\frac{\rho_{nf}\cdot\overline{U}\cdot D}{\mu_{nf}} \quad (9)$$

Also, the empirical relationship for determining the friction factor was:

$$f_{nf}(\exp)=\frac{2\Delta P_{nf}\rho_{nf}D\beta}{G_{nf}^2 nL} \quad (10)$$

ΔP_{nf} is the pressure drop resulting from Eq. (3). All the quantities that were measured to estimate the pressure drop and the friction factor were subjected to uncertainties due to the errors of measurement. The uncertainties of Re_{nf}, pressure drop and friction factor were calculated as 2.8, 3.0 and 2.8%, respectively.

RESULTS AND DISCUSSION

Initially, to ensure reliability of the experimental device, some trials were done for 60%/40% mixture of EG and water at three inlet temperatures of the radiator. Fig. 3 is plotted to validate the experimental values of pressure drop compared to the values obtained using Eq. (4), From this figure, the values of experimental and theoretical pressure drops were in good agreement. The deviation between experimental and calculated ones was less than 8%. To evaluate the effect of various factors on the nanofluid pressure drop flowing through radiator, the experiments were conducted for five volume concentrations (0.05, 0.1, 0.3, 0.5 and 0.8 vol%) and five flow rates (4, 5, 6, 7 and 8 lpm) and also three different inlet temperatures including 35, 44 and 54 °C. Most of the results reported in this study were at 35 °C inlet temperature since the curve trends for two other inlet temperatures (44 and 54 °C) were similar.

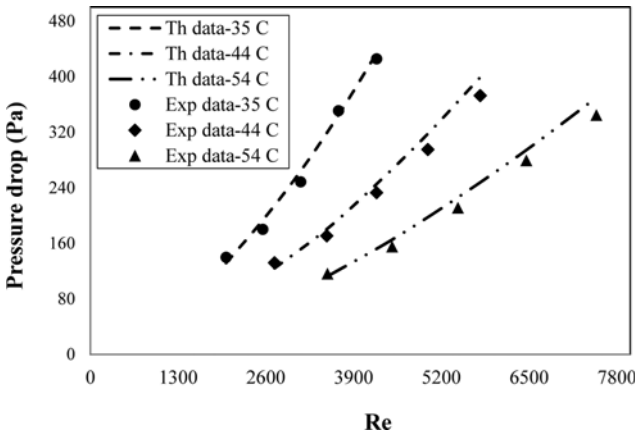

Fig. 3. Comparison between measured pressure drop and that calculated from Eq. (4).

Fig. 4 shows pressure drop variation at 35 °C inlet temperatures versus Reynolds number in different volume concentrations of CuO/EG (60%)-water (40%) nanofluid. As expected, the pressure drop of nanofluid in all tested temperature was higher than that of the base fluid. Also, from this figure, it was concluded that pressure drop increased with Reynolds number as well as volume concentration. For instance, at Re=3100, the pressure drop inside the radiator increased from 287.21 to 344.65 (Pa) with changing volume fraction from 0.05% to 0.8%. In fact, Reynolds number was related

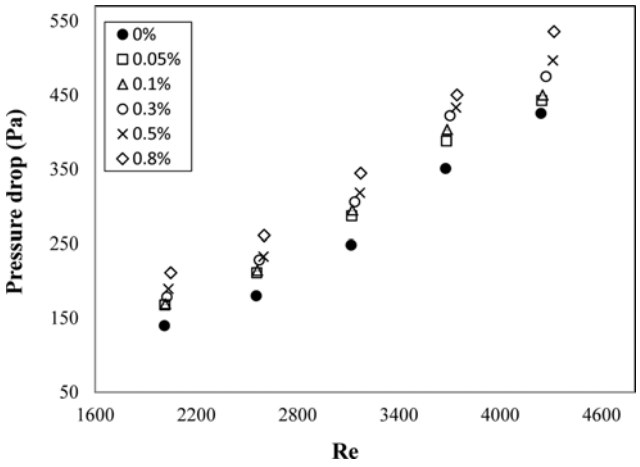

Fig. 4. The effect of Reynolds number and volume concentration on experimental pressure drop (T_{in}=35 °C).

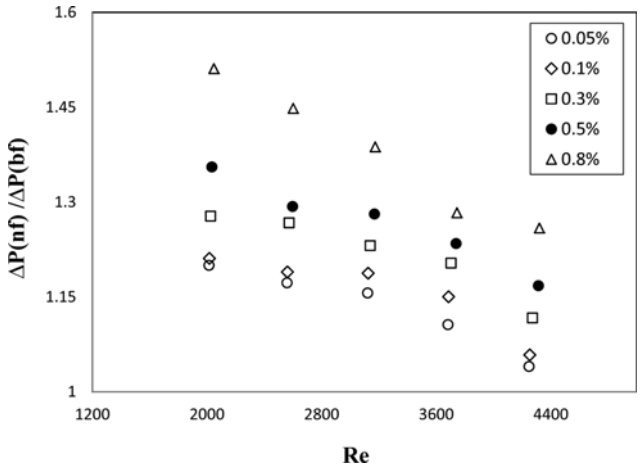

Fig. 5. The ratio of the nanofluid pressure drop to the base fluid pressure drop (T_{in}=35 °C).

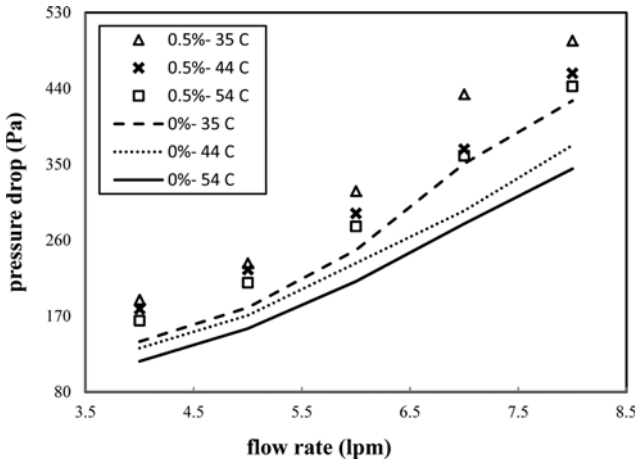

Fig. 6. The effect of inlet flow temperature on pressure drop for base fluid and 0.5 vol% nanofluid flow.

to the length of tube, velocity, viscosity and density of nanofluid in radiator tubes. Considering no changes in the tube length and slight changes in viscosity and density, the main cause which affected pressure drop was the increase in the flow rate in high Reynolds number. Furthermore, suspending solid particles in a fluid generally increased dynamic viscosity relative to the base fluid. Since viscosity was in direct relationship with pressure drop, the larger the value of viscosity, the more growth in pressure drop would occur. In the interim, Brownian motion, dispersion and fluctuation of nanoparticles, especially near the wall of radiator, amplified the momentum exchange rates between the particles. This momentum exchange can considerably increase pressure drop. These results were consistent with those of some other researchers [20,21,30].

The ratio of nanofluid pressure drop to the base fluid pressure drop is illustrated in Fig. 5. Clearly, the increment of Reynolds number resulted in pressure drop ratio decrement. In other words, with increasing Reynolds number for all volume fractions, the role of nanoparticles on nanofluid pressure drop was decreased. By increasing the flow rate in the same volume fraction, the number of nanoparticles per volume was reduced, which led to decrease of apparent viscosity. Also, this pressure drop ratio intensified with increase of volume fraction of nanoparticles at given Reynolds number. The nanoparticles' presence in the base fluid increased viscosity and thus intensified the pressure drop. Since at the lowest volume fraction, the effect of nanoparticles was the least, so the properties of nanofluid were close to base fluid properties, and the lowest proportion of pressure drop could be seen at the lowest volume fraction and the highest Reynolds number. As can be seen in Fig. 5, pressure drop was found to increase by about 15%, 20% and 23% under the same Reynolds number with 0.1%, 0.3% and 0.5% nanofluid concentrations, respectively, compared to the base fluid. Pressure drop of very dilute CuO/water nanofluid flowing through a circular tube was experimentally investigated by Fotukian et al. [24]. According to their study, the value of ($\Delta P_{nf}/\Delta P_{bf}$) increased with nanoparticle concentration. In contrast, Xuan and Li [31] claimed that dilute nanofluid incurred almost no extra penalty of pump power.

Effect of inlet flow temperature on pressure drop for base fluid and 0.5 vol% nanofluid flow is investigated in Fig. 6. By increasing the inlet fluid temperature to radiator, both the output fluid and wall temperature of the radiator increased. This increase of temperature weakened the link of nanoparticles and shrank the size of the nanoparticle clusters, and that would lead to reduced viscosity and thus reduced nanofluid pressure drop. For example, by increasing inlet temperature from 35 °C to 54 °C at the same flow rate (6 lpm), the pressure drop changed from 318.27 to 276.35 (Pa), respectively. So the pressure drop was reduced by about 13.17%.

The experimental friction factor versus Reynolds number at different volume fractions of nanoparticles at 35 °C is plotted in Fig. 7. Evidently, the empirical friction factor decreased with increasing Reynolds number at all nanoparticle volume fractions. According to Eq. (10), the friction factor decreased with increasing velocity. As the Reynolds number ($\rho_{nf}\times\overline{U}\times D_h/\mu_{nf}$) increased, the friction factor decreased dramatically. Also, it can be observed from this figure that the smallest value of friction factor was related to the base fluid, which increased by increasing the concentration of particle volume at given Reynolds number.

For low Reynolds number the friction factor mainly was pro-

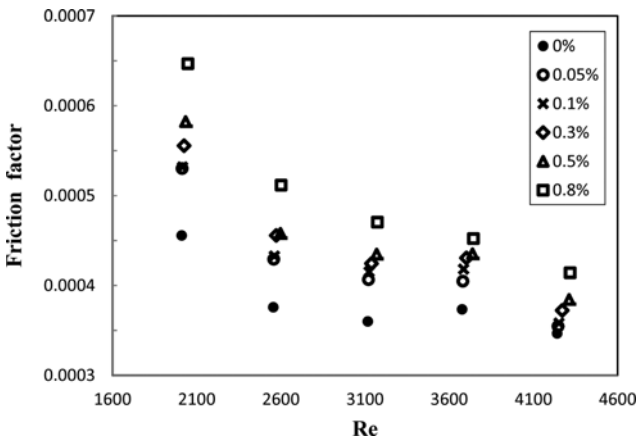

Fig. 7. The effect of concentrations of CuO nanoparticles on friction factor (T_{in}=35 °C).

portional to the fluid viscosity. The other main effects of the nanoparticles inside the fluid 'considering the Brownian motion and fluctuation of the nanoparticles' intensified the momentum transfer between the nanoparticles and base fluid molecules which led to increase the nanofluid friction factor. But at a higher Reynolds number this mechanism was not dominant. In other words, at higher Reynolds number, the friction factor had not considerable dependency on the viscosity of working fluid and flow pattern and velocity played the most important role in increasing the friction factor. Therefore, the effect of viscosity became less pronounced. In the presence of nanoparticles, the difference between nanofluid and base fluid friction factor decreased at higher Reynolds numbers in comparison with lower Reynolds number.

Fig. 8 displays friction factor as a function of flow rate under different inlet temperatures for base fluid and 0.1 vol% nanofluid flow. It is evident that the cluster size of nanoparticles became smaller with increasing average temperature of the fluid caused by the inlet temperature increase. So, a decline was observed in viscosity and pressure drop of nanofluid. During the experiments, the highest reduction in the friction factor was observed for 7 (lpm) flow rate. By increasing the inlet temperature from 35 °C to 54 °C, the friction factor can be decreased about 13.61%.

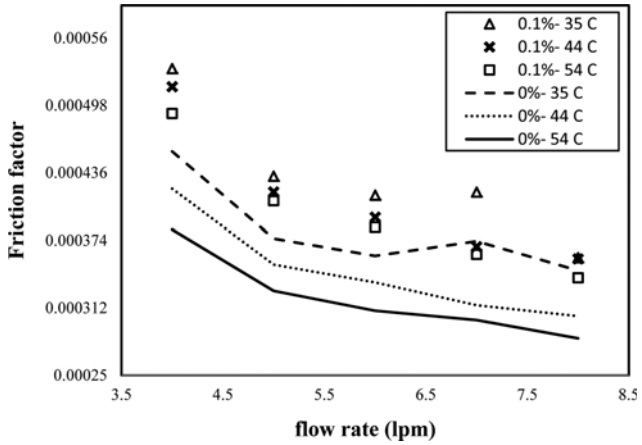

Fig. 8. Comparison of friction factor at different inlet flow temperature of base fluid and 0.1 vol% nanofluid flow.

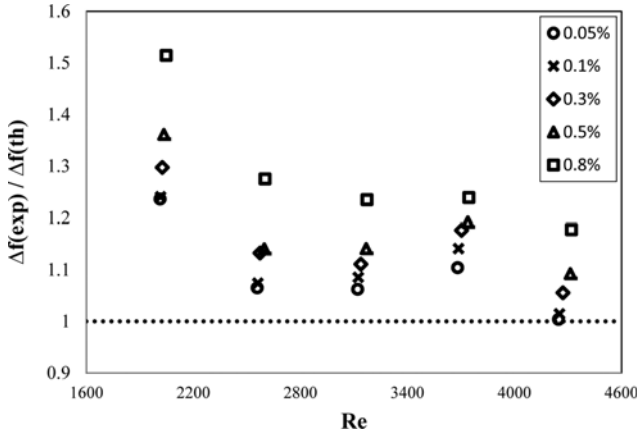

Fig. 9. Comparison of experimental and predicated pressure drop (T_{in}=35 °C).

To determine the ability of theoretical relationship to predict nanofluid behavior, the ratio of experimental friction factor to theoretical one versus Reynolds number is plotted in Fig. 9. This figure indicates that the used pressure drop equation fails to predict friction factor of the nanofluid, which might be because Eq. (10) was applied for single-phase flow and only considered effects of rheological and physical characteristics such as viscosity and density on pressure drop. Generally, the experimental data showed that this equation was not suitable for predicting the friction factor of nanofluid. So, new equations should be provided considering the influence of nanoparticles such as dimensions and volume fraction of nanoparticles, effect of dispersion, browning motion, particle interaction, clustering process, particle emigration and dynamic phase of particles.

Using the present empirical data, the following correlation is derived to estimate the pressure drop of nanofluid flow through the radiator considering the effect of temperature, volume fraction and Reynolds number using least square method of regression analysis.

$$\Delta P_{nf}=11.941\,\mathrm{Re}^{1.33}\,\varphi^{0.412}\,T^{-2.01} \qquad R^2_{adj}=98.3\% \qquad (11)$$

The applicable ranges ar: (i) $0.05\%\le\varphi\le0.8\%$, (ii) $2000\le\mathrm{Re}\le8000$ and (iii) 35 °C≤T≤54 °C. As shown in Fig. 10, the values of pressure drop as predicted by the above correlation were compared with the experimental values and found that they were in the range of between −8% to +14%.

THERMAL PERFORMANCE EVALUATION

Application of nanofluid as a new working media inside the car radiator was investigated by Shokrgozar et al. [32]. Their result showed that by using nanofluid instead of traditional liquid-cooling car radiator, pressure drop and heat transfer increase up to 65% and 55%, respectively. So, is nanofluid effective for enhancing the thermal performance of a car-radiator considering their pressure losses? To find a suitable answer to the question, a performance index (η) is defined as follows [33,34]:

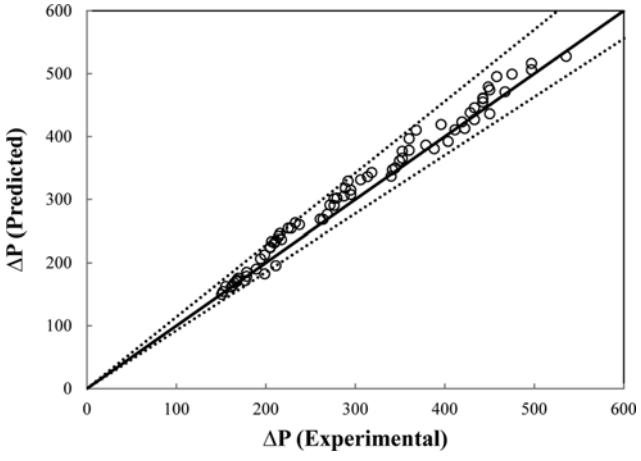

Fig. 10. Comparison of the experimental values for friction factor those predicted by Eq. (11). for nanofluid flow through the radiator.

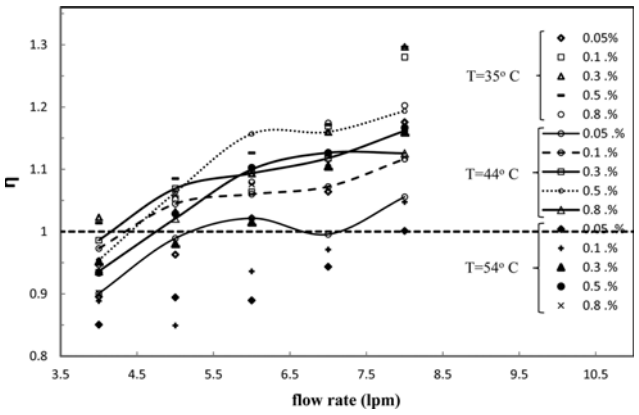

Fig. 11. Performance index values at three different temperatures for the radiator inlet fluid (EG (60%)-water (40%)/CuO).

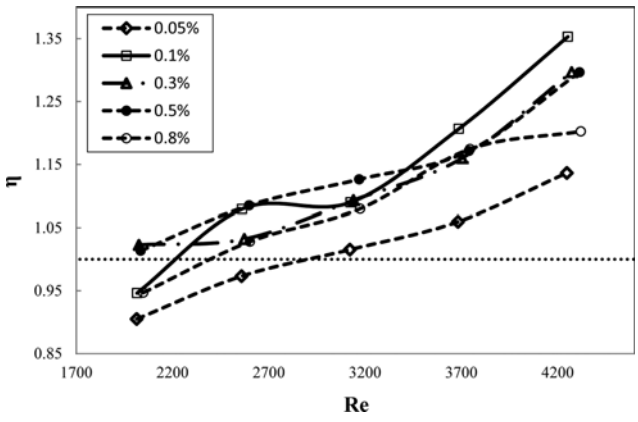

Fig. 12. Performance index values for EG (60%)-water (40%)/CuO nanofluid (T_{in}=35 °C).

$$\eta = \frac{h_{nf}/h_{bf}}{\Delta P_{nf}/\Delta P_{bf}} = \frac{R_h}{R_{\Delta P}} \quad (12)$$

in which, R_h is the ratio of heat transfer enhancement by application of nanofluid instead of common liquid-cooling car radiator and $R_{\Delta P}$ $R_{\Delta P}$ is the ratio of nanofluid pressure drop to the base fluid one. Apparently, when the performance index is greater than unity, it implies that application of nanofluid in a car is more in the favor of heat transfer enhancement rather than in the favor of pressure drop increasing. In Fig. 11, performance index for CuO/EG (60%)-Water (40%) nanofluid based on the flow rate and under three inlet temperature is shown. As it can be concluded from this figure, by increasing the flow rate, the performance index increased at the same inlet temperature. For most of the nanofluid concentrations, the performance index was greater than one, indicating that application of nanofluids at higher flow rate is an appropriate way to increase the thermal ability of car-radiator fluids.

The values of the performance index for each inlet temperature, concentration, and three flow rates are reported in Table 3. As shown, with increasing the nanofluid concentrations, the performance index did not show the same trend. Although heat transfer was enhanced by increasing the nanoparticle content of fluids, but the pressure drop through the radiator intensified too. For example, while the nanofluid concentration changed from 0.05 to 0.3 vol% at 54 °C and 6 lpm, the performance index increased from 0.089 to 1.014, but with adding more nanoparticles to the fluid, the performance index decreased.

Table 3. Performance index values at three different temperatures and three flow rates

Flow rate (lpm)	T(in) \ φ	0.05%	0.1%	0.3%	0.5%	0.8%
5	35 °C	0.963	1.053	1.032	1.084	1.028
	44 °C	0.989	1.044	1.069	1.062	1.020
	54 °C	0.894	0.849	0.980	1.028	1.057
6	35 °C	1.021	1.063	1.093	1.126	1.079
	44 °C	1.021	1.060	1.093	1.156	1.099
	54 °C	0.889	0.936	1.014	1.102	1.075
7	35 °C	1.064	1.169	1.159	1.171	1.174
	44 °C	0.995	1.072	1.117	1.160	1.126
	54 °C	0.943	0.971	1.104	1.126	1.110

The performance index at 35 °C for different volume fraction of nanoparticles is plotted in Fig. 12. From this figure it can be obviously concluded that nanofluid showed better performance at higher Reynolds numbers. On the one hand, when the nanofluid concentration was larger than 0.1%, the pressure drop of nanofluid flows in the radiator increased dramatically. On the other hand, in concentrations of less than 0.1%, the presence of nanoparticles could not change the heat transfer rate of the radiator in comparison to the base fluid considerably. It means that at 0.1% concentration of nanofluid, the positive effects of heat transfer enhancement overcame the negative effects of pressure loss of nanofluid flow. So the best performance was achieved in 0.1% concentration of nanofluid.

CONCLUSIONS

CuO nanoparticles with 60 nm average diameter were added to a mixture of 60/40 EG and water to investigate the effects of different parameters on pressure drop of nanofluid flows in PRIDE-radiator. The pressure drop and friction factor of nanofluid through the radiator with volume concentration of less than 0.8% were measured at five flow rate (4, 5, 6, 7, 8 lpm). The experimental results are as follows:

- Pressure drop increased in the presence of nanoparticles compared to the base fluid. This trend is intensified by increasing both Reynolds number and volume fraction of nanoparticles, which is due to increasing viscosity.
- With increasing inlet fluid temperature to radiator, both the output fluid and temperature of the radiator increased. This increase of temperature reduces viscosity of nanofluid and leads to decrease of pressure drop and friction factor. When the inlet temperature increased by 19 °C, pressure drop was reduced by about 13.17%.
- The ratio of pressure drop of nanofluid to that of base fluid is decreased with Reynolds number at a given volume fraction of nanoparticles.
- The friction factor is the least for the base fluid, increasing with rising volume fraction and decreasing by increasing of Reyn-

olds number.

• An empirical correlation was proposed for pressure drop of nanofluid in the car radiator, which predicted the present experimental data within an error band of −8% and +14%.

• For each inlet temperature, with increasing flow rate, the performance index went upward and indicated that application of nanofluid in higher flow rate was affordable.

NOMENCLATURE

A : cross section the tube [m^2]
D : inner diameter of tube [m]
ΔP : pressure drop [Pa]
f : friction factor
G : mass velocity [kg/m^2s]
L : tube length of radiator [m]
g : specific gravity [m/s^2]
Re : Reynolds number
Δh : change in liquid height inside the capillary [m]
n : number of tube passes
T : temperature [°C]
$\overline{U}$: velocity [m/s]
$\dot{m}$: mass flow rate [kg/s]
h : heat transfer coefficient [W/m^2K]

Greek Symbols

β : viscosity correction factor
η : performance index
μ : viscosity [kg/m·s]
ρ : density [kg/m^3]
σ : minimum free flow area/frontal area
φ : volume concentration of nanoparticle

Subscripts

bf : basefluid
exp : experimental
fr : frontal
in : input
lam : laminar
lpm : liter/min
nf : nanofluid
out : output
p : particle
th : theoretical
turb : turbulant
w : tube wall

REFERENCES

1. S. U. S. Choi, *ASME FED 231/MD*, **66**, 99 (1995).
2. S. M. Peyghambarzadeh, S. H. Hashemabadi, S. M. Hoseini and M. SeifiJamnani, *Int. Commun. Heat Mass*, **38**, 1283 (2011).
3. M. Hojjat, S. Gh. Etemad and R. Bagheri, *Korean J. Chem. Eng.*, **27**, 1391 (2010).
4. S. Zeinali Heris, S. Gh. Etemad and M. N. Esfahany, *Int. Commun. Heat Mass*, **33**, 529 (2006).
5. S. M. S Murshed , K. C. Leong, C. Yang and N. Nguyen, *Int. J. Nanoscience*, **7**, 325 (2008).
6. M. Kahani, S. Zeinali Heris and S. M. Mousavi, *J. Disper. Sci. Technol.*, **34**, 1704 (2013).
7. M. Emami Meibodi, M. Vafaie-Sefti, A. M. Rashidi, A. Amrollahi, M. Tabasi and H. Sid Kalal, *Int. Commun. Heat Mass*, **37**, 319 (2010).
8. S. M. Hashemi and M. A. Akhavan-Behabadi, *Int. Commun. Heat Mass*, **39**, 144 (2012).
9. B. H. Chun, H. U. Kang and S. H. Kim, *Korean J. Chem. Eng.*, **25**, 966 (2008).
10. M. Raji Asadabadi, H. Abolghasemi, M. Ghannadi Maragheh and P. Davoodi Nasab, *Korean J. Chem. Eng.*, **30**, 733 (2013).
11. M. Nasiri, S. Gh. Etemad and R. Bagheri, *Korean J. Chem. Eng.*, **28**, 2230 (2011).
12. D. P. Kulkarni, R. S. Vajjha, D. K. Das and D. Oliva, *Appl. Therm. Eng.*, **25**, 1774 (2008).
13. K. Y. Leong, R. Saidur, S. N. Kazi and A. H. Mamun, *Appl. Therm. Eng.*, **30**, 2685 (2010).
14. T. P. Teng, Y. H. Hung, C. S. Jwo, C. C. Chen and L. Y. Jeng, *Particuology*, **9**, 486 (2011).
15. S. K. Das, N. Putra and W. Roetzel, *Int. J. Heat Mass Transfer*, **46**, 851 (2003).
16. Y. Rao, *Particuology*, **8**, 549 (2010).
17. W. J. Tseng and K. C. Lin, *Mater. Sci. Eng.*, **355**, 186 (2003).
18. U. Rea, T. McKrell, L. W. Hu and J. Buongiorno, *Int. J. Heat Mass Transfer*, **52**, 2042 (2009).
19. P. C. Mukesh Kumar, J. Kumar and S. Suresh, *J. Mech. Sci. Technol.*, **27**, 239 (2013).
20. W. Duangthongsuk and S. Wongwises, *Int. J. Heat Mass Transfer*, **52**, 2059 (2009).
21. J. Lee and I. Mudawar, *Int. J. Heat Mass Transfer*, **50**, 452 (2007).
22. M. N. Pantzali, A. G. Kanaris, K. D. Antoniadis, A. A. Mouza and S. V. Paras, *Int. J. Heat Fluid Flow*, **30**, 691 (2009).
23. M. Boudouh, H. L. Gualous and M. D. Labachelerie, *Appl. Therm. Eng.*, **30**, 2619 (2010).
24. S. M. Fotukian and M. Nasr Esfahany, *Int. Commun. Heat Mass*, **37**, 214 (2010).
25. Y. He, Y. Jin, H. Chen, Y. Ding, D. Cang and H. Lu, *Int. J. Heat Mass Transfer*, **50**, 2272 (2007).
26. G. H. Ko, K. Heo, K. Lee, D. S. Kim, C. Kim, Y. Sohn and M. Choi, *Int. J. Heat Mass Transfer*, **50**, 4749 (2007).
27. T. Sun and A. S. Teja, *J. Chem. Eng. Data, Transfer*, **48**, 198 (2003).
28. B. C. Pak and I. Y. Cho, *Exp. Heat Transfer*, **11**, 151 (1998).
29. D. A. Drew and S. L. Passman, *Theory of multi component fluids*, Springer, Berlin (1999).
30. K. V. Sharma, L. S. Sundar and P. K. Sarma, *Int. Commun. Heat Mass*, **36**, 503 (2009).
31. Y. Xuan and Q. Li, *J. Heat Transfer*, **125**, 151 (2003).
32. M. Shokrgozar, S. Zeinali Heris, S. Pourfarhang, M. Shanbedi and S. H. Noie, *J. Disper. Sci. Technol.*, **35**, 677 (2014).
33. L. J. Brognaux, R. L. Webb, L. M. Chamra and B. Y. Chung, *Int. J. Heat Transfer*, **40,** 4345 (1997).
34. M. Kahani, S. Zeinali Heris and S. M. Mousavi, *Powder Technol.*, **246**, 82 (2013).